Catalytic Reaction Profile for Alcohol Oxidation by Galactose Oxidase†

Mei M. Whittaker and James W. Whittaker*

Department of Biochemistry and Molecular Biology, Oregon Graduate Institute of Science and Technology, 20000 Northwest Walker Road, Beaverton, Oregon 97006-8921

Received February 13, 2001; Revised Manuscript Received May 3, 2001

ABSTRACT: Galactose oxidase is a remarkable enzyme containing a metalloradical redox cofactor capable of oxidizing a variety of primary alcohols during enzyme turnover. Recent studies using 1-*O*-methyl α-D-galactopyranoside have revealed an unusually large kinetic isotope effect (KIE) for oxidation of the α-deuterated alcohol ($k_H/k_D = 22$), demonstrating that cleavage of the 6,6′-di[^{2}H]hydroxymethylene C−H bond is fully rate-limiting for oxidation of the canonical substrate. This step is believed to involve hydrogen atom transfer to the tyrosyl phenoxyl in a radical redox mechanism for catalysis [Whittaker, M. M., Ballou, D. P., and Whittaker, J. W. (1998) *Biochemistry 37*, 8426−8436]. In the work presented here, the enzyme's unusually broad substrate specificity has allowed us to extend these investigations to a homologous series of benzyl alcohol derivatives, in which remote (meta or para) substituents are used to systematically perturb the properties of the hydroxyl group undergoing oxidation. Quantitative structure−activity relationship (QSAR) correlations over the steady state rate data reveal a shift in the character of the transition state for substrate oxidation over this series, reflected in a change in the magnitude of the observed KIE for these reactions. The observed KIE values have been shown to obey a log−linear correlation over the substituent parameter, Hammett σ. For the relatively difficult to oxidize nitro derivative, the KIE is large ($k_H/k_D = 12.3$), implying rate-limiting C−H bond cleavage for the oxidation reaction. This contribution becomes less important for more easily oxidized substrates (e.g., methoxy derivatives) where a much smaller KIE is observed ($k_H/k_D = 3.6$). Conversely, the solvent deuterium KIE is vanishingly small for 4-nitrobenzyl alcohol, but becomes significant for the 4-methoxy derivative ($k_{H_2O}/k_{D_2O} = 1.2$). These experiments have allowed us to develop a reaction profile for substrate oxidation by galactose oxidase, consisting of three components (hydroxylic proton transfer, electron transfer, and hydrogen atom transfer) comprising a single-step proton-coupled electron transfer mechanism. Each component exhibits a distinct substituent and isotope sensitivity, allowing them to be identified kinetically. The proton transfer component is unique in being sensitive to the isotopic character of the solvent (H_2O or D_2O), while hydrogen atom transfer (C−H bond cleavage) is independent of solvent composition but is sensitive to substrate labeling. In contrast, electron transfer processes will in general be less sensitive to isotopic substitution. Our results support a mechanism in which initial proton abstraction from a coordinated substrate activates the alcohol toward inner sphere electron transfer to the Cu(II) metal center in an unfavorable redox equilibrium, forming an alkoxy radical which undergoes hydrogen atom abstraction by the tyrosine−cysteine phenoxyl free radical ligand to form the product aldehyde.

Galactose oxidase is a fungal metalloenzyme, a radical−copper oxidase (*1*−*3*), that catalyzes oxidation of primary alcohols to the corresponding aldehydes and reduction of O_2 to hydrogen peroxide (*4*):

$$RCH_2OH + O_2 \rightarrow RCHO + H_2O_2 \qquad (1)$$

The enzyme exhibits an unusually broad specificity for reductant, and a wide variety of primary alcohols serve as effective substrates, including substituted benzyl alcohols (*5*). The physiological substrate for the extracellular enzyme is unknown, and the canonical substrate (galactose) is actually a poorer substrate than a simpler alcohol, dihydroxyacetone. The broad substrate specificity allows the enzyme to metabolize a wide range of alcohols in the environment to efficiently generate hydrogen peroxide, the biologically important product.

The catalytic mechanism of galactose oxidase has attracted considerable interest, particularly in light of unusual features of the active site structure that have been revealed by spectroscopic (*1*−*3*, *6*, *7*) and crystallographic (*8*, *9*) studies (Figure 1). In its active form, the enzyme contains a novel protein free radical coordinated to a Cu(II) metal center forming a radical−copper complex whose special reactivity serves as a paradigm for metalloradical catalysis in the rapidly expanding field of free radical enzymology (*10*−*12*). The stabilized free radical in galactose oxidase is localized on a tyrosyl side chain, covalently modified by cross-linking to a cysteinyl residue to form a tyrosine−cysteine dimer in the protein (Tyr 272−Cys 228) (*8*, *9*). The enzyme supports a ping-pong turnover reaction (Scheme 1) where substrate (alcohol) binds to the active enzyme radical−

† Support for this project from the National Institutes of Health (Grant GM 46749 to J.W.W.) is gratefully acknowledged.

* Corresponding author. Telephone: (503) 748-1065. Fax: (503) 748-1464. E-mail: jim@bmb.ogi.edu.

10.1021/bi010303l CCC: $20.00 © 2001 American Chemical Society
Published on Web 05/23/2001

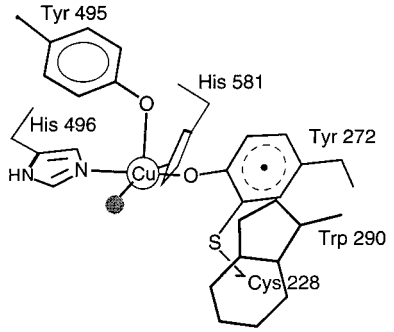

FIGURE 1: Active site of galactose oxidase, based on crystallographic data (PDB entry 1gog). A gray sphere identifies the exogenous ligand (solvent or small molecule) binding site.

Scheme 1

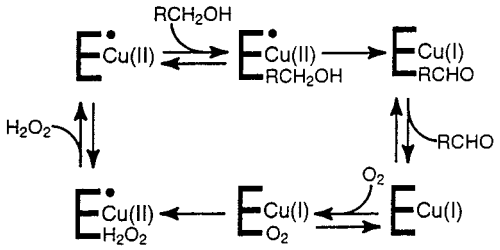

copper complex in the first half-reaction, reducing both sites. In the second half-reaction, dioxygen binds and is reduced to hydrogen peroxide. This basic mechanism has been established by steady state kinetic analysis (*13*, *14*), and is further supported by results from rapid reaction studies (*15*, *16*). Reduction and oxidation half-reactions occur on very different time scales, the O_2 reaction being nearly 1000-fold faster ($k_{red} = 1.5 \times 10^4$ M^{-1} s^{-1}; $k_{ox} = 8.0 \times 10^6$ M^{-1} s^{-1}) (*15*). As a result, the reaction with reducing substrate is rate-limiting at low substrate concentrations. The active site is quite open, and interactions with the substrates are weak ($K_{m,Gal} = 150$ mM) and nonspecific, resulting in formation of what may be described as essentially collisional substrate complexes. Isotopic labeling experiments have demonstrated that substrate oxidation proceeds by stereospecific abstraction of the *pro-S* hydrogen of the hydroxymethylene functional group (*17*), and the large deuterium kinetic isotope effect (KIE)[1] associated with this reaction ($k_H/k_D = 10-22$) (*15*) implies that C−H bond cleavage is fully rate-limiting. However, a number of questions remain regarding the details of the alcohol oxidation reaction. In particular, the ordering of single-electron transfer (SET) and hydrogen atom transfer (HAT) steps in the oxidation mechanism and their relative contributions to the transition state are still unresolved. Also, the relation between these two processes and substrate activation by proton abstraction is unclear.

The unusual tolerance that galactose oxidase exhibits toward variations in substrate structure has allowed us to investigate these questions by systematically varying the substrate and correlating these structural features with catalytic efficiency. A homologous series of monosubstituted benzyl alcohols (Scheme 2, X = F, Cl, Br, I, SCH_3, H, CH_3, CF_3, NO_2, or OCH_3; Y = F, Cl, Br, OCH_3, or NO_2) has been used to probe the substrate dependence of the enzymatic reaction. Quantitative structure−activity relationships (QSARs) and isotope kinetics, which have proven to be powerful tools for probing other enzymatic redox mechanisms (*18*−*25*), provide the framework for analyzing these results, yielding significant new insights into the enzyme oxidation processes.

Scheme 2

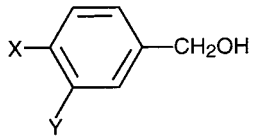

MATERIALS AND METHODS

Biological Materials. Galactose oxidase was isolated from *Dactylium dendroides* as previously described (*1*, *26*). Recombinant galactose oxidase was prepared by high-density methanolic fermentation of a *Pichia pastoris* transformant containing multiple copies of a chromosomally integrated expression cassette consisting of the *Aspergillus niger* glucoamylase signal peptide (gla) fused to the cDNA sequence encoding the mature galactose oxidase protein (GAOX) under the AOX1 promoter. The recombinant enzyme was purified and converted to the catalytically active form as previously described (*27*).

Synthesis of 3- and 4-Substituted Benzyl Alcohol Substrates. The compounds comprising the homologous series of benzyl alcohols used in this work were synthesized as the protio (deuterio) forms by borohydride (borodeuteride) reduction of commercially available precursors. Method A involved reduction of benzoyl ester by lithium borohydride (*28*). Typically, 12 mmol of lithium bromide was added to 12 mmol of sodium borohydride in 15 mL of 2-methoxy ethyl ether (diglyme) and the mixture stirred at room temperature. After 30 min, 20 mmol of benzoyl ester was added to the reaction flask and the mixture heated in an oil bath (100 °C) for ≥3 h. The progress of the reaction was monitored by silica gel TLC developed in a hexane/ethyl acetate (1:1) solvent. When the reaction was complete, the sample was poured into 25 mL of ice-cold 10% hydrochloric acid. For benzyl alcohol products having melting points of >25 °C, the crystalline product was collected from the acid solution and recrystallized from hot water. For lower-melting point products, the reaction mixture was extracted with methylene chloride and the product was purified by silica gel column chromatography (1:1 hexane/ethyl acetate mixture) and fractionally distilled under vacuum. Method B involved reduction of benzoyl ester by calcium borohydride in tetrahydrofuran at room temperature (*29*). Anhydrous calcium chloride (25 mmol) was triturated into a solution of 50 mmol of sodium borohydride in 30 mL of anhydrous tetrahydrofuran. The benzoyl ester (25 mmol) was added to the mixture and stirred for 8−20 h. The progress of the reaction was monitored, and the product was isolated as described above. Method C proceeded from substituted benzoic acid, esterified by stirring in methanol with Dowex 50X2-400 ion-exchange resin under reflux for 24 h, as previously described (*30*). The resulting methyl ester was subsequently reduced by sodium borohydride as described above (method A). All compounds were verified by GC−MS: (a) 3-bromo benzyl alcohol via method A, (b) 3-chloro

[1] Abbreviations: GAOX, galactose oxidase; HAT, hydrogen atom transfer; KIE, kinetic isotope effect; PT, proton transfer; QSAR, quantitative structure−activity relationship; SET, single-electron transfer; SKIE, solvent kinetic isotope effect; TS, transition state.

benzyl alcohol via method A, (c) 3-fluoro benzyl alcohol via method A, (d) 3-methoxy benzyl alcohol via method A, (e) 3-nitro benzyl alcohol via method B, (f) 4-bromo benzyl alcohol via method A, (g) 4-chloro benzyl alcohol via method A, (h) 4-fluoro benzyl alcohol via method A, (i) 4-iodo benzyl alcohol via method C, (j) 4-methoxy benzyl alcohol via method A, (k) 4-methyl benzyl alcohol via method A, (l) 4-methylthio benzyl alcohol via method A, (m) 4-nitro benzyl alcohol via method B, and (n) 4-trifluoromethyl benzyl alcohol via method A. All other compounds were from commercial sources and were used without further purification.

Enzyme Assay. Enzyme activity was measured using a thermostated (25 °C) Clark oxygen electrode connected to a high-accuracy polarographic amplifier (*15*). Reactions were carried out in 50 mM Na_2HPO_4 buffer (pH 7) with 5 mM benzyl alcohol substrate and 0.24 mM O_2 (air-saturated). In addition, 2 mM $K_3Fe(CN)_6$ was routinely included in the reaction buffer to maintain the active state of the enzyme. For absolute rate measurements, the response of the Clark oxygen electrode was calibrated on the basis of the stoichiometric oxygen consumption in the protocatechuic acid/protocatechuate dioxygenase reaction (*15*, *31*). Briefly, 0.1 μmol of protocatechuic acid was added to the reaction buffer in a thermostated cell, and the full amplitude of oxygen uptake was recorded following addition of an excess (approximately 50 units) of *Brevibacterium fuscum* protocatechuate dioxygenase (*31*). Protocatechuate dioxygenase was prepared from *B. fuscum* (ATCC 15993) as previously described (*31*). For isotope effect measurements, protio and deuterio forms of a given substrate were assayed in parallel. Substrates were dissolved in assay buffer by sonication, and the concentrations of the corresponding isotopic samples were checked by UV absorption spectroscopy. Slight differences in substrate concentration detected by absorption measurements were typically corrected by adjusting the volumes of the substrate stock solution in the assay mixture according to the intensity of the UV spectra for the two samples.

Data Analysis. Model correlations were investigated and statistically evaluated using the program QSAR-PC (*32*). The kinetic data input for the analysis were the average of triplicate determinations. Standard values and definitions were used for reactivity, electronic, and structural parameters [Hammett σ (σ_p^+, σ_m), molecular refractivity (MR), and steric constant (E_S)] (*33*, *34*).

RESULTS

Galactose oxidase metabolizes all of the 3- and 4-substituted benzyl alcohol derivatives that were tested, with an approximately 20-fold maximum variation in relative rates. All of the benzyl alcohol derivatives that were tested served as simple substrates, yielding linear oxygen uptake kinetics. These results demonstrate that turnover-based inactivation of the enzyme, which would be reflected in deviations from linear O_2 uptake in these experiments, is insignificant for incubation over the course of at least 2 min with these substrates even in the absence of oxidant [e.g., $K_3Fe(CN)_6$]. This behavior is very similar to that observed for the canonical substrate, galactose, in the enzyme assay. All of the rate data described below were obtained from initial slopes, making any slower inactivation process irrelevant, and ferricyanide was routinely included in the assay buffers for galactose oxidase to ensure that the enzyme was fully active during the kinetic measurements.

Table 1: Kinetic Parameters for Oxidation of Benzyl Alcohol Derivatives by Galactose Oxidase

substituent	k_H (M^{-1} s^{-1})	k_D (M^{-1} s^{-1})	k_H/k_D
4-OCH_3	449 ± 2	123.8 ± 1.1	3.63 ± 0.04
4-SCH_3	862 ± 7	182.6 ± 1.4	4.72 ± 0.05
4-CH_3	322 ± 2	64.2 ± 1.4	5.02 ± 0.11
4-F	177 ± 2	26.5 ± 0.5	6.67 ± 0.14
4-H	424 ± 2	60.5 ± 0.7	7.00 ± 0.09
4-Cl	460 ± 2	67.4 ± 0.7	6.84 ± 0.08
4-I	800 ± 5	132.2 ± 1.4	6.06 ± 0.07
4-Br	587 ± 5	91.2 ± 1.1	6.44 ± 0.16
4-CF_3	383 ± 2	44.0 ± 0.5	8.71 ± 0.10
4-NO_2	324 ± 2	26.3 ± 0.5	12.33 ± 0.23
3-OCH_3	4172 ± 14	1011.4 ± 2.3	4.12 ± 0.02
3-F	1213 ± 7	206.4 ± 0.7	5.88 ± 0.04
3-Cl	2186 ± 16	349.2 ± 1.8	6.26 ± 0.06
3-Br	2109 ± 2	312.0 ± 2.7	6.76 ± 0.06
3-NO_2	662 ± 7	60.5 ± 0.5	10.94 ± 0.14

The limited solubility of the benzyl alcohol series of compounds in buffered aqueous solution constrains the concentration range over which kinetic measurements can be performed. For the relatively soluble 3-methoxy benzyl alcohol, the turnover rate was found to be linear in substrate concentration up to 55 mM benzyl alcohol (data not shown). This implies that $K_m > 100$ mM for the benzyl substrates and that substrate oxidation is rate-limiting for enzyme turnover at benzyl alcohol concentrations of up to 50 mM. [For comparison, the K_m for the canonical substrate, galactose, is 150 mM (*35*), and the K_m for acetol, an α-keto alcohol that supports the highest catalytic turnover rate known for galactose oxidase, is estimated to be 1.4 M (*36*).] The low substrate concentrations (5 mM benzyl alcohol derivative) used in the investigation of turnover rates for the homologous substrate series ensure that the substrate oxidation half-reaction was rate-limiting in these experiments.

The initial-rate reaction velocities (v_0) measured for galactose oxidase turnover at these low substrate concentrations ([S] $\ll K_m$) were used to estimate the catalytic efficiency, using an approximation ($v_0/[S] \approx V_{max}/K_m$) that is valid in the linear limit of the hyperbolic substrate saturation curve, where the reaction becomes essentially bimolecular. For subsequent analysis, this result was further divided by the enzyme concentration, converting it to an effective second-order rate constant (k_H and k_D, respectively, for protio and deuterio substrates), corresponding approximately to k_{cat}/K_m for the enzymatic reaction.

Initial-rate steady state oxygen uptake kinetic data for the para-substituted series of benzyl alcohol substrates are listed in Table 1. The range of reaction rate constants measured for this series was remarkably narrow, varying only 4-fold over the entire set of protio compounds and less than 2-fold for the compounds at the extreme values of the electronic substituent parameter, Hammett σ_p. Plotting the data as a function of σ_p^+ (Figure 2, H) yields a small, negative reaction parameter ρ of -0.093 ± 0.32. The large standard deviation for the correlation is a consequence of the empirical scatter of the kinetic constants around the single-parameter regression line, and is not the result of poor statistics for the individual rate constant determinations. A similar correlation

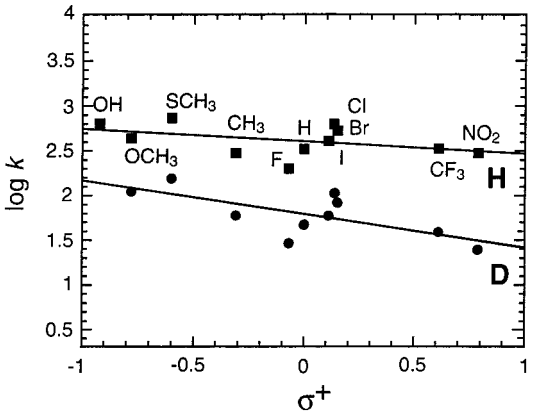

FIGURE 2: QSAR correlations for para-substituted benzyl alcohols. Rate data for galactose oxidase turnover supported by protio (■) or deuterio (●) benzyl alcohols are shown in a semilog linear free energy plot vs the electronic substituent parameter Hammett σ_p^+. The slopes of the correlation lines are as follows: $\rho_H = -0.09 \pm 0.32$ and $\rho_D = -0.49 \pm 0.61$.

Table 2: Rate Correlations for Oxidation of Benzyl Alcohol Derivatives

parameter	correlation slope	intercept	correlation coefficient	F^a	rmsd
	(A) Para-Substituted α,α-[$^1H_2$]BA				
σ_p^+	-0.093 ± 0.32	2.64 ± 0.15	0.22	0.42	0.208
MR	0.038 ± 0.002	2.37 ± 0.16	0.84	19.1	0.116
$\sigma_p^+ +$ MR	-0.070 ± 0.29 (σ_p^+)	2.38 ± 0.17	0.85	8.85	0.121
	0.038 ± 0.002 (MR)				
E_S	-0.068 ± 0.24	2.57 ± 0.29	0.22	0.40	0.208
$\sigma_p^+ + E_S$	-0.165 ± 0.59 (σ_p^+)	2.56 ± 0.31	0.31	0.38	0.217
	-0.107 ± 0.29 (E_S)				
	(B) Para-Substituted α,α-[$^2H_2$]BA				
σ_p^+	-0.489 ± 0.61	1.91 ± 0.21	0.54	3.32	0.254
MR	0.047 ± 0.034	1.50 ± 0.28	0.74	9.75	0.202
$\sigma_p^+ +$ MR	-0.500 ± 0.29 (σ_p^+)	1.57 ± 0.18	0.93	20.9	0.122
	0.048 ± 0.02 (MR)				
E_S	-0.012 ± 0.35	1.82 ± 0.42	0.03	0.01	0.301
$\sigma_p^+ + E_S$	-0.650 ± 0.68 (σ_p^+)	1.77 ± 0.35	0.63	2.34	0.250
	-0.166 ± 0.33 (E_S)				
	(C) Meta-Substituted α,α-[$^1H_2$]BA				
σ_m	-1.297 ± 0.94	3.74 ± 0.40	0.91	14.5	0.144
MR	0.030 ± 0.15	3.05 ± 0.99	0.31	0.33	0.330
$\sigma_m +$ MR	-1.336 ± 0.46 (σ_m)	3.53 ± 0.27	0.99	35.5	0.070
	0.037 ± 0.03 (MR)				
E_S	0.526 ± 2.1	2.86 ± 2.4	0.37	0.46	0.475
$\sigma_m + E_S$	-2.36 ± 0.69 (σ_m)	3.00 ± 0.34	0.99	51.2	0.086
	-0.406 ± 0.47 (E_S)				
	(D) Meta-Substituted α,α-[$^2H_2$]BA				
σ_m	-2.02 ± 0.9	3.21 ± 0.39	0.96	38.4	0.137
MR	0.025 ± 0.02	2.27 ± 1.5	0.17	0.1	0.502
$\sigma_m +$ MR	-2.05 ± 0.46 (σ_m)	3.00 ± 0.27	0.99	77.8	0.070
	0.035 ± 0.03 (MR)				
E_S	-0.526 ± 2.1	2.86 ± 1.9	0.37	0.46	0.475
$\sigma_m + E_S$	-2.356 ± 0.69 (σ_m)	3.00 ± 0.34	0.99	51.24	0.086
	-0.41 ± 0.48 (E_S)				

[a] The F value is a test statistic relating the residuals of each point to the regression line to the residuals of each point to the mean value of the data. The F value depends on the number of variables and data points, and a larger value of F indicates a more significant correlation.

for rate constants measured for the corresponding deuterio compounds (Figure 2, D) yields a slightly larger value of -0.49 ± 0.61. For comparison, bilinear correlations were also investigated over alternative substituent parameters, MR and E_S (Table 2). The correlation was slightly improved by including a second parameter in the fit, with an increase in the correlation coefficient for the protio series from 0.22 (for σ_p^+ alone) to 0.85 (for $\sigma_p^+ +$ MR) with an increase in $F_{1,8}$ from 0.4 to 19. A similar increase was found for the bilinear correlation over the deuterio series (Table 2). However, in both cases, the component of the correlation slope attributed to σ_p^+ is essentially unchanged. Including the purely steric parameter E_S did not improve the correlation.

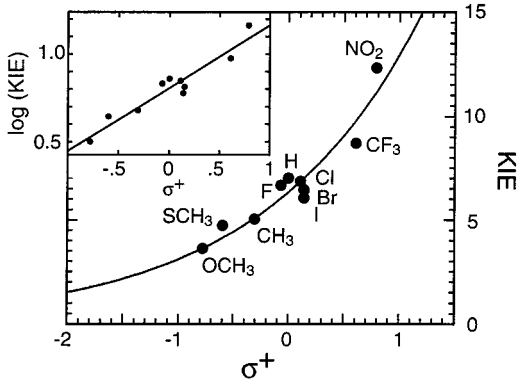

FIGURE 3: Substituent dependence of the deuterium KIE for substrate oxidation. The observed k_H/k_D rate ratio for the para-substituted homologues is plotted vs the electronic substituent parameter Hammett σ_p^+. The inset is a semilog representation of the same data.

The deuterium KIEs for substrate oxidation in the para-substituted series of benzyl alcohols are evaluated in Table 1 and plotted as a function of σ_p^+ in Figure 3. In contrast to the relatively uniform values found for the rates, the observed KIEs show a strong trend with values rapidly increasing at larger σ values. The experimental data were fit to an exponential function [Figure 3 (—)], and the log−linear correlation of the KIEs is further demonstrated in the inset. The results of a quantitative investigation of the correlation between log(KIE) and Hammett σ are given in Table 3. The $F_{1,8}$ value for the correlation implies significance in the >99.9% confidence interval.

More dramatic variations in rates were observed for the meta-substituted substrate series (Table 1). In this case, the protio substrate oxidation rates spanned a 7.5-fold range, and correlation with Hammett σ_m (Figure 4) yielded a relatively large, negative reaction parameter ρ of -1.3 ± 0.9. An even steeper slope is obtained for the deuterio compound correlations, corresponding to a reaction parameter ρ of -2.0 ± 0.9. As found for the para-substituted series, bilinear correlations (particularly with MR) provide some overall improvement but do not change the fundamental results. Once again, the KIEs for substrates available in both protio and deuterio forms follow a trend toward larger isotope effects associated with larger σ values (Figure 5). This trend also can be fit as an exponential function as shown, leading to a log−linear correlation with σ_m (Figure 5, inset). Statistical analysis of the log(KIE) correlation for the meta series of compounds implies significance at the >99.9% confidence interval.

The sensitivity of the oxidation rates for four of the para-substituted substrates to isotopic solvent was also investigated in these experiments. The substrates chosen for this experiment span a range of rates and represent the full range of the substituent parameter σ_p^+ explored in these studies. A small deuterium solvent isotope effect (SKIE) was found for the oxidation of 4-nitrobenzyl alcohol ($k_{H_2O}/k_{D_2O} = 1.05 \pm 0.03$), with progressively larger values observed for the

Table 3: Logarithmic Correlation of KIEs with Substituent Parameters

substituent position	parameter	correlation slope	intercept	correlation coefficient	*F*	rmsd
para	σ_p^+	0.428 ± 0.14	0.738 ± 0.047	0.92	47.2	0.059
meta	σ_m	0.694 ± 0.17	0.543 ± 0.075	0.99	120.	0.027

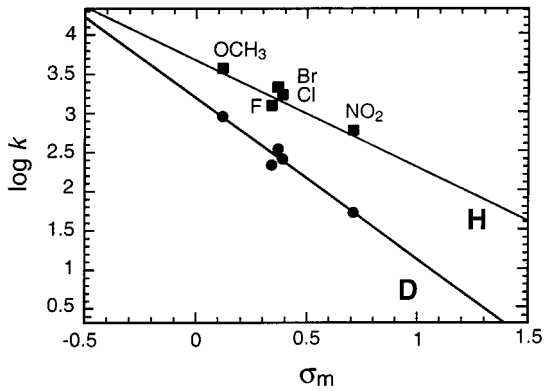

FIGURE 4: QSAR correlations for meta-substituted benzyl alcohols. Rate data for galactose oxidase turnover supported by protio (■) or deuterio (●) benzyl alcohols are shown in a semilog linear free energy plot vs the electronic substituent parameter Hammett σ_m. The slopes of the correlation lines are as follows: $\rho_H = -1.30 \pm 0.94$ and $\rho_D = -2.0 \pm 0.9$.

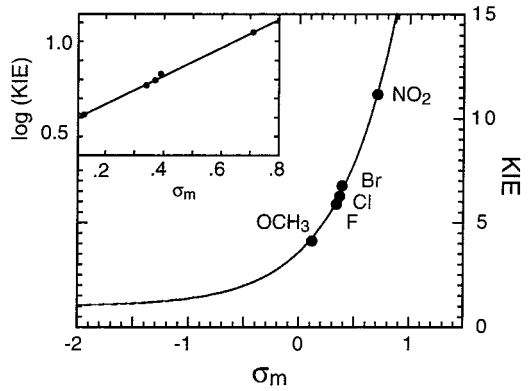

FIGURE 5: Substituent dependence of the deuterium KIE for substrate oxidation. The observed k_H/k_D rate ratio for the meta-substituted homologues is plotted vs the electronic substituent parameter Hammett σ_m. The inset is a semilog representation of the same data.

4-trifluoromethyl ($k_{H_2O}/k_{D_2O} = 1.11 \pm 0.01$), 4-H ($k_{H_2O}/k_{D_2O} = 1.16 \pm 0.02$), and 4-methoxy ($k_{H_2O}/k_{D_2O} = 1.22 \pm 0.02$) derivatives. The correlation between the substrate KIE for oxidation of each of these benzyl alcohol derivatives with the solvent deuterium KIE for the same substrates is shown in Figure 6.

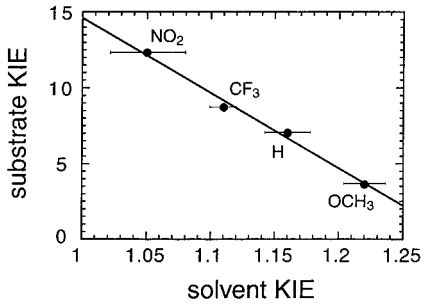

FIGURE 6: Correlation of the substrate and solvent KIEs for benzyl alcohol oxidation. The horizontal bars indicate the magnitude of the standard deviations.

DISCUSSION

In general terms, detailed studies of enzyme catalysis may be approached by modifying the structure of either the protein or the substrate. Site-directed mutagenesis has been widely used to alter the structure of enzyme active sites to assign roles to individual residues and provide a clearer view of their catalytic functions. However, mutagenesis can fundamentally change active site reactivity, often with unpredictable results. Alternatively, the substrate itself can be systematically varied to reveal more subtle features of the enzyme interactions by perturbing the energetic profile for the catalytic complexes. The latter approach, coupled with quantitative structure−reactivity analysis of the kinetic consequences, has proven to be valuable in studies of cytochrome P450 (*19*, *20*) and flavoenzyme monooxygenase (*21*−*23*) and oxidase (*24*) mechanisms, and is the basis of the work presented here. In contrast to the generally unpredictable consequences of protein mutagenesis, the effects of substituents on the properties of reactive functional groups are generally highly predictable.

The success of the substrate-variation method hinges on the ability of the enzyme to accept a range of aryl substrates representing a wide variety of substituents. It is also important that steric effects on the reaction be relatively small so that the electronic factors controlling the oxidation mechanisms will be clearly expressed. Fortunately, the unusually broad substrate specificity of galactose oxidase allows us to systematically explore a range of structures within a homologous series of benzyl alcohols, with substituents ranging from strongly electron-donating to strongly electron-withdrawing groups. Although these compounds are only distantly related structurally to the canonical substrate, galactose, they closely resemble a number of natural products (e.g., veratryl alcohol) that may serve as physiological substrates for galactose oxidase.

Catalytic oxidation rate constants for the homologous substrates (Table 1) show uniform log−linear correlations over the empirical free energy parameter (Hammett σ) that defines the magnitude of the substituent perturbation (Figure 2). For the para-substituted benzyl alcohols, the trends are similar for either σ_p or σ_p^+, and the correlation with σ_p^+ shown in Figure 2 is representative. The σ_p^+ parameter has been found to be appropriate for a variety of oxidation reactions, particularly where radical intermediates are involved (*37*). The rate correlations show no sign of break points that would indicate a change in mechanism or a transition between discrete rate-limiting steps in a multistep reaction. The largest deviations from the model occur in the halogen series, which form a subset of substituents within a narrow range of σ_p^+ values showing a strong trend [$k_H(F) < k_H(Cl) < k_H(Br) < k_H(I)$] that is clearly independent of σ_p^+, while the other substituents, including 4-nitro, closely conform to the model. Clearly, while electronic perturbations described by Hammett σ_p^+ dominate the behavior shown in

Scheme 3

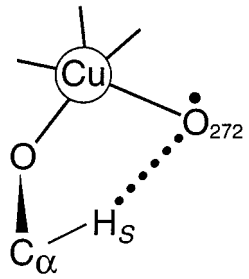

Figure 2, other factors are likely to contribute to substrate interactions, and the correlations are, in fact, improved by including additional parameters (MR and E_S) in a multilinear QSAR analysis (Table 2).

The most important features of the plots shown in Figure 2 are the slopes of the correlation lines, which correspond to the sensitivity of the reaction to the substituent perturbation. The small, negative value of the correlation slope for the protio benzyl alcohols corresponds to a value for Hammett ρ of $\approx$0, characteristic of a reaction controlled by an uncharged transition state that is relatively insensitive to the stabilizing effects of electron-withdrawing or -donating substituents. In the limit of small correlation slope ρ, the correlation coefficient and F value, as measures of covariance of the dependent and independent variables, must vanish. The small values that we find for these test statistics in the analysis of our data (Table 2) thus support the σ_p^+ independence of the data, a property that has significant mechanistic implications (see below).

The ρ value describing the correlation of properties with the electronic parameter Hammett σ plays an important role in the analysis of reaction mechanisms, since it contains information about the nature of the transition state (*33*, *34*, *37*). Insensitivity of a reaction to varying values of σ_p^+ is generally regarded as the signature of a free radical or atom-abstraction oxidation mechanism, characterized by an absence of charge buildup on the benzylic carbon (Cα) in the transition state, or a cyclic transition state that avoids charge separation (*37*). The flat correlation found experimentally for the galactose oxidase alcohol oxidation reaction (Figure 2) is consistent with the previously proposed radical mechanism for catalysis (*1*−*3*, *15*). The insensitivity to σ_p^+ may also reflect a cyclic transition state for the oxidation process, as shown in Scheme 3. This five-atom cyclic transition state brings the phenoxyl oxygen of the Tyr 272 free radical near the hydrogen atom that is removed from the substrate Cα during turnover (*2*, *3*, *15*). The slight negative value found for ρ in these experiments suggests that oxidation is facilitated by electron-donating groups in the para position. For comparison, a similar ρ of −0.14 has been reported for Hammett analysis of benzyl alcohol oxidation by an enzyme-inspired phenoxyl−Cu(II) catalyst (*38*).

The correlation with molecular refractivity (MR) that is revealed in a bilinear analysis of the galactose oxidase alcohol oxidation rate data (Table 2) is also suggestive. Molecular refractivity is an empirical parameter relating to the high-frequency electronic polarizability, defined by the Lorentz−Lorenz equation:

$$\mathrm{MR} = [(n^2 - 1)/(n^2 + 2)](\mathrm{MW}/d) \qquad (2)$$

Scheme 4

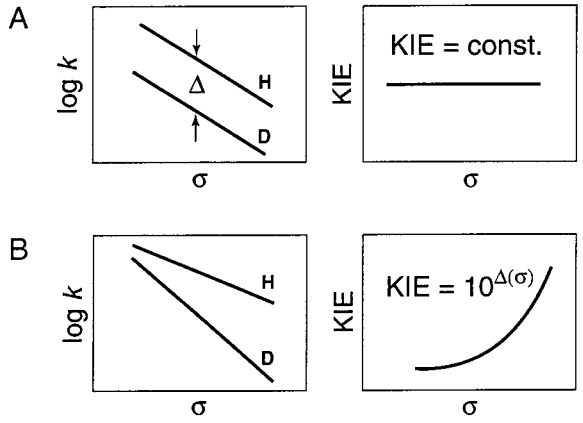

where n is the refractive index, MW the molecular weight, and d the density (*33*, *34*). This parameter cross-correlates with steric and hydrophobic parameters, but is intrinsically electronic in origin, relating to the HOMO/LUMO splitting in the valence shell of the molecule. The existence of a correlation between oxidation rates and MR may imply involvement of a low-lying electronic excited state in the electron transfer mechanism.

Curiously, the slope (ρ) found for the rate correlation over deuterio alcohols differs from that found for the protio series (Figure 2), associated with a strong substituent dependence of the kinetic isotope effect (Figure 3). The entire substitution series can be fit with an exponential dependence of the KIE on Hammett σ, further demonstrated by the log−linear plot shown in the inset. While dropping the result for the 4-nitro derivative might appear to allow a linear (rather than exponential) KIE curve, the nitro compound does *not* exhibit anomalous behavior in either of the rate correlations (Figure 2, H and D), so there is no justification for distinguishing it in the KIE analysis (also, see below). In any case, the substituent dependence of the KIE is a clear indication of *a change in the character of the transition state* over the reaction series, since the fundamental reaction is the same for each of these substrates.

While rate correlations are well-established mechanistic tools, KIE correlations have not been as extensively developed. The underlying relation between rate and KIE correlations is illustrated in Scheme 4, which shows idealized views of two limiting cases. For a transition state whose essential character is unchanged through a reaction series, protio and deuterio correlations will give the same value of ρ, and appear as parallel lines on the Hammett plot (Scheme 4A). The separation between the two correlation lines, Δ, is related to the KIE for the reaction:

$$\Delta = \log k_H - \log k_D = \log \mathrm{KIE} \qquad (3)$$

No substituent dependence of the KIE will be observed in this limit, since KIE $= 10^{\Delta(\sigma)} =$ a constant. This limit has previously been observed in the oxidation of benzylamine substrate analogues by the flavoenzyme monoamine oxidase A (*21*). On the other hand, divergent correlation lines for protio and deuterio compounds (Scheme 4B) imply an exponential dependence of the KIE on substituent parameters, explaining the behavior of the KIEs for the para substitution series, shown in Figure 3. This limit has previously been

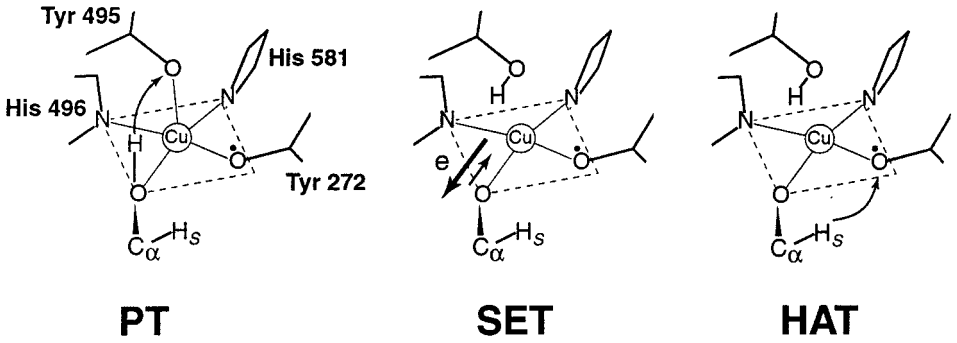

FIGURE 7: Resolved elementary components of the galactose oxidase substrate oxidation reaction.

observed in oxidative reactions of P450, where it was used to make an empirical identification with oxyradical oxidation chemistry exhibiting the same substituent KIE dependence (*18*). Although isotope effect data for oxidation of benzyl alcohols by phenoxyl radicals are very limited, it is interesting to note that the KIE found for oxidation of α,α-[$^2H_2$]-benzyl alcohol by a small molecule phenoxyl−Cu(II) complex that mimics galactose oxidase reactivity (k_H/k_D = 6.8) (*39*) is similar to that observed for oxidation of the same substrate by the enzyme (Table 1).

The substituent dependence of the KIE is a very sensitive expression of shifts in the character of the transition state under perturbations. Because the KIE ratio eliminates nonelectronic contributions to the reactivity (each pair being identical except for the isotopic substitution), the quality of the correlation of the KIE with σ_p^+ (Table 3 and Figure 3) is strikingly better than that found for the individual rate constants (k_H and k_D) which may be influenced by other factors contributing to the scatter in the data (Table 2 and Figure 2). Scheme 4 demonstrates that the linear substituent correlations, well-established for reaction rates, *require* log−linear KIE correlations over the same parameters if the isotopic substrate correlations are distinct. Thus, there are physical reasons to expect a logarithmic dependence of KIE on σ, while there is no obvious basis for a linear relation.

Similar trends are observed for the meta substitution series (Figures 4 and 5). In this case, a larger correlation slope is observed for the rates, suggesting that the presence of a meta substituent on the aromatic ring may alter the geometry of the substrate complex, leading to a transition state structure distinct from that found for the para series. This is not particularly surprising, since the meta substituent is closer to the functional group undergoing reaction and, as a consequence, might be more likely to encounter steric interference in the active site. In support of this interpretation, benzyl alcohol (3-H) deviates strongly from the other members of this set, while it correlates well with the para series. An exponential substituent dependence of the KIE is also found for the meta series.

While the substituent-dependent KIE for the reaction reflects a change in the transition state, the absence of a break in the rate correlation indicates the underlying mechanism is unchanged. This, in turn, implies that substrate oxidation represents a single kinetic step comprised of several components, distinguished by their isotope and substituent sensitivities. Substrate oxidation by galactose oxidase is equivalent to dehydrogenation of the alcohol hydroxymethylene group, the elements of H_2 being transferred to redox centers and basic sites in the enzyme. This reaction may be described as a complex proton-coupled electron transfer process, involving two electrons and two protons. To understand how the transition state for the reaction will be affected when the substituents are varied, it is useful to identify three elementary processes [proton transfer (PT), single-electron transfer (SET), and hydrogen atom transfer (HAT)] that may comprise the oxidation step (Figure 7).

The relatively acidic hydroxylic proton of the coordinated substrate is expected to undergo abstraction by a general base in the active site in a simple proton transfer process (Figure 7, PT) (*7*, *40*). The hydroxylic proton exchanges rapidly with solvent protons in aqueous solution, being replaced by a deuteron in D_2O. The OH group is distinct in this regard, and no other sites in the substrate are expected to exchange. As a result, rate-limiting PT is predicted to give rise to a significant SKIE. The absence of a measurable SKIE in the reaction with galactose (*15*) indicates that, in that case at least, PT does not contribute significantly to the transition state for oxidation. On the other hand, proton abstraction by an active site base (Tyr 475 tyrosinate) has been proposed as an essential (but non-rate-limiting) substrate activation step (*7*, *40*), a role which has been supported by subsequent mutagenesis studies (*41*).

Single-electron transfer (Figure 7, SET) is a second component of the substrate oxidation reaction. This elementary process is facilitated by orbital overlaps between the coordinated alcohol and Cu(II) in the inner sphere substrate complex. The overall driving force for SET is the difference in potential between enzyme sites and the substrate in the catalytic complex, which is determined by the substrate oxidation potential in a reaction profile like that developed in these experiments (see below). While an electronic process like SET will not exhibit a primary kinetic isotope effect, it may contribute to an overall reaction KIE through an equilibrium isotope effect resulting from the change in bond order for both methylene C−H bonds on oxidation of the deprotonated alkoxide to a neutral alkoxyl radical. The fractionation factor (the perturbation of the redox equilibrium by isotopic substitution) would then multiply the intrinsic KIE for the subsequent C−H bond cleavage step (*15*).

Hydrogen atom transfer (Figure 7, HAT) between the coordinated substrate and the Tyr 272 tyrosyl phenoxyl in the active site is the third key feature of a free radical alcohol oxidation mechanism for galactose oxidase (*1*−*3*, *15*). HAT involves cleavage of the C−H bond α to the alcohol hydroxyl, and is therefore sensitive to isotopic substitution in the substrate. Primary and secondary kinetic isotope effects (associated with the scissile and nonscissile α C−H bonds, respectively) will in general both contribute to an overall

KIE, and these two are not resolved in the experiments described here using α-di[^{2}H]alcohols. A primary KIE will generally lie in the range of 3−10, with the larger value being associated with a transition state in which C−H bond breaking dominates. On the basis of the magnitude of the primary deuterium KIE measured in both steady state and rapid kinetics studies, the HAT process appears to be fully rate-limiting for oxidation of galactose (*15*). HAT processes depend on special geometric constraints on donor and acceptor sites, as well as electronic factors relating to the driving force for the reaction.

In the context of the study presented here, these three elementary processes (which are not necessarily associated with distinct kinetic intermediates) provide a framework for understanding the reaction profile revealed by systematically varying the substrate. The large deuterium KIE observed for benzyl alcohols bearing electron-withdrawing substituents (e.g., NO_2 and CF_3) indicates that C−H bond cleavage is likely to be fully rate-limiting for oxidation of those compounds. As previously found for galactose oxidation, no excess SKIE is detected when the reaction is performed in D_2O, and since the PT and HAT processes can be resolved in this case, the two components are clearly not concerted. With more electron-releasing substituents, the substrate KIE becomes progressively smaller, complemented by an increase in the SKIE, which reaches a value of maximum of 1.22 for 4-methoxy benzyl alcohol, whose substrate KIE is a minimum value for the series. This does not appear to simply reflect a decrease in the acidity of the hydroxyl group, since oxidation of the even more basic C_6-alkoxyl group in galactose yields a *smaller* SKIE (0.99 ± 0.05) and *larger* substrate KIE ($k_H/k_D = 24$) (*15*), corresponding to values near the *y*-intercept of the KIE/SKIE correlation for the benzyl alcohol substrates (Figure 6). The SKIE for the reaction of the 4-methoxy derivative is significant, but smaller than the SKIEs ($k_{H_2O}/k_{D_2O} = 3-5$) reported for reactions where PT is fully rate-limiting (*42*). Thus, the transition state associated with substrate oxidation for the benzyl alcohols bearing electron-*donating* substituents is more consistent with an SET process, with some PT contribution (based on the observation of a significant SKIE), while substrates bearing electron-*withdrawing* substituents are limited by HAT.

While the Hammett σ correlations provide a useful empirical framework for investigating substituent perturbations, substrate oxidation is expected to be specifically sensitive to the redox potential of the alcohol, which defines the thermodynamic driving force ($\Delta G = -nFE$) for the reaction. In Marcus theory, it also controls the rate by affecting the height of the reaction barrier. The correlation of oxidation rate and KIE versus ionization potential (E_{ox}) for the para-substituted series of benzyl alcohols is shown in Figure 8, using E_{ox} values based on anodic oxidation of the alcohols (*43*). The rates show a relatively weak dependence on the ionization potential, similar to the results shown in Figure 2, reflecting the cross-correlation between ionization potential and σ_p, although the slight trend toward a more rapid reaction for the more reducing substrates is, in fact, in the direction expected on the basis of driving force considerations.

The strong variation in KIE with ionization potential is mechanistically more significant. As shown qualitatively in

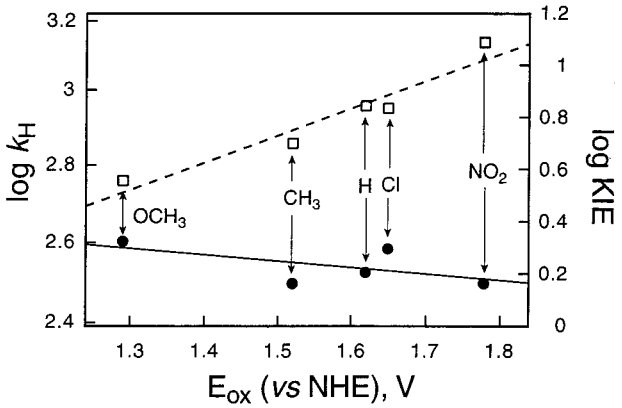

FIGURE 8: Correlation of log rate or log KIE for oxidation of benzyl alcohol substrates with anodic ionization potentials. Rates for protio alcohol oxidation (●) and KIE (□) (ionization potentials from ref 43).

Scheme 5

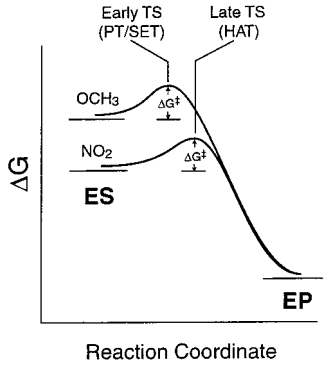

Scheme 5, a change in the driving force for a reaction will in general produce a shift in the transition state. The difference in ionization potentials for 4-methoxy and 4-nitro benzyl alcohols implies a substantial (~95 kJ/mol) difference in driving force for oxidation of these two alcohols by galactose oxidase. Although the activation barriers ($\Delta G^{\ddagger}$) must be nearly the same, since the rates are similar, the transition states (TSs) will be different. In particular, the TS for the reaction with the larger driving force (oxidation of the methoxy derivative) is predicted to occur earlier along the reaction coordinate than that for oxidation of the nitro compound. The large KIE observed for oxidation of 4-nitro benzyl alcohol indicates the TS is dominated by C−H bond cleavage in that reaction, while the relatively small substrate KIE and increasing SKIE are consistent with PT and SET dominating the earlier TS for 4-methoxy benzyl alcohol oxidation. In addition to providing insight into energetic aspects of substrate oxidation, correlation of the rates and KIEs with ionization potentials allows extension of the analysis beyond the aromatic alcohol series for which Hammett σ is defined. For a simple primary alkanol (such as ethanol or the C-6 hydroxyl of galactose) which is even more difficult to oxidize (E_{ox} ~ 2.4 V vs NHE) (*44*), we would predict an even larger substrate KIE and no SKIE, as has been experimentally observed for galactose oxidation (*15*).

The combination of isotope kinetics and substrate-level perturbations of the active site thus resolves the elementary processes in the galactose oxidase oxidation mechanism, revealing the essential chemistry of the radical−copper complex. These experiments effectively map out a profile

of the substrate oxidation reaction by systematically varying the nature of the substrate. The simultaneous and complementary expression of substrate and solvent KIEs in these reactions (Figure 6) without a corresponding break in the rate profile (Figure 2) suggests that PT, SET, and HAT events are not associated with distinct kinetic intermediates but rather represent asynchronous components of a single kinetic step. The changing sensitivity of the oxidation reaction to deuteration of the α-position over the homologous substrate series then reflects a shift in the character of the transition state from rate-limiting C−H bond cleavage to rate-limiting proton abstraction-activated SET in the reaction profile, shown by the emergence of a significant SKIE in the latter limit. We are led to a picture of a complex reaction coordinate for substrate oxidation by galactose oxidase in which PT, SET, and HAT components all occur consecutively in a single kinetically resolvable step, i.e., no energetic barriers $\geq kT$ separate these events along the reaction coordinate. Within this reactivity spectrum, the electronic properties of the substrate determine which contributions dominate the overall transition state for alcohol oxidation.

REFERENCES

1. Whittaker, M. M., and Whittaker, J. W. (1988) *J. Biol. Chem. 263*, 6074−6080.
2. Whittaker, J. W. (1994) in *Metal Ions in Biological Systems* (Sigel, H., Ed.) Vol. 30, pp 315−360, Marcel Dekker, New York.
3. Whittaker, J. W., and Whittaker, M. M. (1998) *Pure Appl. Chem. 70*, 903−910.
4. Avigad, G., Amaral, D., Asensio, C., and Horecker, B. L. (1962) *J. Biol. Chem. 237*, 2736−2743.
5. Kosman, D. J. (1984) in *Copper Proteins and Copper Enzymes* (Lontie, R., Ed.) Vol. 2, pp 1−26, CRC Press, Boca Raton, FL.
6. Whittaker, M. M., and Whittaker, J. W. (1990) *J. Biol. Chem. 265*, 9610−9613.
7. Whittaker, M. M., Ekberg, C. A., Peterson, J., Sendova, M. S., Day, E. P., and Whittaker, J. W. (2000) *J. Mol. Catal. B: Enzym. 8*, 3−15.
8. Ito, N., Phillips, S. E. V., Stevens, C., Ogel, Z. B., McPherson, M. J., Keen, J. N., Yadav, K. D. S., and Knowles, P. F. (1991) *Nature 350*, 87−90.
9. Ito, N., Phillips, S. E. V., Yadav, K. D. S., and Knowles, P. F. (1994) *J. Mol. Biol. 238*, 794−814.
10. Stubbe, J., and van der Donk, W. A. (1998) *Chem. Rev. 98*, 705−762.
11. Frey, P. A. (1997) *Curr. Opin. Chem. Biol. 1*, 347−356.
12. Pedersen, J. Z., and Finazzi-Agro, A. (1993) *FEBS Lett. 325*, 53−58.
13. Hamilton, G. A., de Jersey, J., and Adolf, P. K. (1973) in *Oxidases and Related Redox Systems* (King, T. E., Mason, H. S., and Morrison, M., Eds.) Vol. 1, pp 103−124, University Park Press, Baltimore.
14. Villafranca, J. J., Freeman, J. C., and Kotchevar, A. (1993) in *Bioinorganic Chemistry of Copper* (Karlin, K. D., and Tyeklar, Z., Eds.) pp 439−446, Chapman and Hall, New York.
15. Whittaker, M. M., Ballou, D. P., and Whittaker, J. W. (1998) *Biochemistry 37*, 8426−8436.
16. Borman, C. D., Saysell, C. G., and Sykes, A. G. (1997) *J. Biol. Inorg. Chem. 2*, 480−487.
17. Maradufu, A., Cree, G. M., and Perlin, A. S. (1971) *Can. J. Chem. 49*, 3429−3437.
18. Manchester, J. I., Dinnocenzo, J. P., Higgins, L., and Jones, J. P. (1997) *J. Am. Chem. Soc. 119*, 5069−5070.
19. Higgins, L., Bennett, G. A., Shimoji, M., and Jones, J. P. (1998) *Biochemistry 37*, 7039−7046.
20. Vaz, A. D., and Coon, M. J. (1994) *Biochemistry 33*, 6442−6449.
21. Miller, J. R., and Edmondson, D. E. (1999) *Biochemistry 38*, 13670−13683.
22. Yorita, K., Misaki, H., Palfey, B. A., and Massey, V. (2000) *Proc. Natl. Acad. Sci. U.S.A. 97*, 2480−2485.
23. Oritz-Maldonado, M., Gatti, D., Ballou, D. P., and Massey, V. (1999) *Biochemistry 38*, 16636−16647.
24. Menon, V., Hsieh, C.-T., and Fitzpatrick, P. F. (1995) *Bioorg. Chem. 23*, 42−53.
25. Sobrado, P., Daubner, S. C., and Fitzpatrick, P. F. (2001) *Biochemistry 40*, 994−1001.
26. Tressel, P. S., and Kosman, D. J. (1982) *Methods Enzymol. 89*, 163−171.
27. Whittaker, M. M., and Whittaker, J. W. (2000) *Protein Expression Purif. 20*, 105−111.
28. H. C., Mead, E. J., and Rao, B. C. S. (1955) *J. Am. Chem. Soc. 77*, 6209−6213.
29. Dvorken, L. V., Smyth, R. B., and Mislow, K. (1957) *J. Am. Chem. Soc. 79*, 486−492.
30. Bollenback, G. N. (1963) in *Methods in Carbohydrate Chemistry*, (Whistler, R. L., and Wolfrom, M. L., Eds.) Vol. 2, pp 326−328, Academic Press, New York.
31. Whittaker, J. W., Orville, A. O., and Lipscomb, J. D. (1990) *Methods Enzymol. 188*, 82−88.
32. Coburn, R. A. (1989) *QSAR-PC. A Microcomputer Program for Drug Design*, BIOSOFT, Cambridge, MA.
33. Hansch, C., and Leo, A. (1995) *Exploring QSAR. Fundamentals and Applications in Chemistry and Biology*, American Chemical Society, Washington, DC.
34. Hansch, C., and Leo, A. (1995) *Exploring QSAR. Hydrophobic, Electronic, and Steric Constants*, American Chemical Society, Washington, DC.
35. Driscol, J. J., and Kosman, D. J. (1985) in *Biological and Inorganic Copper Chemistry* (Karlin, K. D., and Zubieta, J., Eds.) pp 75−82, Adenine Press, New York.
36. Kwiatkowski, L. D., Adelman, M., Pennely, R., and Kosman, D. J. (1981) *J. Inorg. Biochem. 14*, 209−222.
37. Gilliom, R. D. (1970) *Introduction to Physical Organic Chemistry*, p 214, Addison-Wesley, New York.
38. Wang, Y., DuBois, J. L., Hedman, B., Hodgson, K. O., and Stack, T. D. P. (1998) *Science 279*, 537−540.
39. Itoh, S., Taki, M., Takayama, S., Nagatomo, S., Kitagawa, T., Sakurada, N., Arakawa, R., and Fukuzumi, S. (1999) *Angew. Chem., Int. Ed. 38*, 2774−2776.
40. Whittaker, M. M., and Whittaker, J. W. (1993) *Biophys. J. 64*, 762−772.
41. Reynolds, M. P., Baron, A. J., Wilmot, C. M., Phillips, S. E. V., Knowles, P. F., and McPherson, M. J. (1995) *Biochem. Soc. Trans. 23*, 510S.
42. Schowen, K. B., and Schowen, R. L. (1982) *Methods Enzymol. 87*, 551−606.
43. Morita, M., Kitamura, S., Ishikawa, M., and Matsuda, Y. (1996) *Electroanalysis 8*, 826−830.
44. Che, C.-M., Tang, W.-T., Lee, W.-O., Wong, K.-Y., and Lau, T.-C. (1992) *J. Chem. Soc., Dalton Trans.*, 1551−1556.

BI010303L